

CMB lensing and scale dependent new physicsAlireza Hojjati^{1,2} and Eric V. Linder³¹*Department of Physics and Astronomy, University of British Columbia, Vancouver V6T 1Z1, British Columbia, Canada*²*Physics Department, Simon Fraser University, Burnaby V5A 1S5, British Columbia, Canada*³*Berkeley Center for Cosmological Physics & Berkeley Lab, University of California, Berkeley, California 94720, USA*

(Received 5 August 2015; published 27 January 2016)

Cosmic microwave background lensing has become a new cosmological probe, carrying rich information on the matter power spectrum and distances over the redshift range $z \approx 1 - 4$. We investigate the role of scale dependent new physics, such as from modified gravity, neutrino mass, and cold (low sound speed) dark energy, and its signature on CMB lensing. The distinction between different scale dependences, and the different redshift dependent weighting of the matter power spectrum entering into CMB lensing and other power spectra, imply that CMB lensing can probe simultaneously a diverse range of physics. We highlight the role of arcminute resolution polarization experiments for distinguishing between physical effects.

DOI: [10.1103/PhysRevD.93.023528](https://doi.org/10.1103/PhysRevD.93.023528)**I. INTRODUCTION**

Gravitational lensing of the cosmic microwave background radiation (CMB lensing) is a recently measured, powerful cosmological probe. The primordial photons are deflected by mass concentrations along the line of sight, sampling the matter density power spectrum—and the laws of gravity—over the entire cosmic history from recombination to the present. While this rearrangement of photons has long been recognized, with early papers accounting for the key elements of both the dispersive and coherent nature of the scattering, and its dependence on the matter power spectrum, dating to the 1980s [1–4], the first statistically significant detection in the CMB alone was in 2011 [5].

The lensing smears out the photon temperature power spectrum, but also induces non-Gaussianity, generating nontrivial four-point correlations [6,7], and a form of parity violation, converting between E -mode (parity even) and B -mode (parity odd) polarization [8]. These effects have now all been detected [5,9–18].

From these observed effects one forms the CMB lensing power spectrum, a measure of the lensing strength as a function of the multipole, or angular scale. This will be the tool we focus on in this paper to explore new physics. One can compare this to, in the first instance, complete lack of lensing (i.e. verifying that lensing exists), and then for example, to the power predicted in the Λ CDM model as a test of the cosmology. Current constraints on the CMB lensing power spectrum include [10,12,16,19,20].

With the first measurements, the statistical significance of detection relative to a null result was the main result. This was often quoted in terms of the ratio of the measured lensing power relative to that predicted in the concordance cosmological constant plus cold dark matter (Λ CDM)

cosmology fit from the temperature power spectrum: $A_{\text{lens}} = C^{dd}/C_{\Lambda\text{CDM}}^{dd}$ [21]. Now that measurements of the lensing power spectrum have dramatically improved, to signal to noise levels greater than 40, the characterization of the detailed power spectrum is of interest.

While one might consider the amplitude of the lensing power as a measure of the overall growth of matter clustering, this is not quite true: the lensing power spectrum is a projection from many redshifts, hence the growth rate effectively enters, and over many wave numbers to a given angular multipole ℓ , so that nonlinear density evolution can enter even at low, ostensibly linear ℓ . Thus any change in cosmology should exhibit a different angular dependence than in the given concordance model, at some level. This implies that A_{lens} becomes scale dependent.

Moreover, when scale dependent growth arises even in the linear density regime, we expect a correspondingly stronger signature of scale dependence (relative to Λ CDM) in the CMB lensing power spectrum. Thus, CMB lensing can act as a probe of such physics, i.e. modified gravity with its scalaron Compton wavelength, neutrino mass with its free streaming scale, or clustering dark energy with its sound horizon.

Indeed, the authors of [10] recently measured A_{lens} in several bins of ℓ (see their Table 1 and Fig. 6; also see Fig. 34 of [22]) with mild hints of scale dependence. Increased accuracy, especially from ongoing high resolution, ground based polarization experiments such as the Atacama Cosmology Telescope [23], POLARBEAR/Simons Array [24], and the South Pole Telescope [25], and the next generation CMB-S4, will place constraints on such scale dependent effects.

In Sec. II we review the basic relation of the CMB lensing power spectrum to the matter power spectrum and

gravitational coupling strength. We present a simple analytic expression to motivate intuition for the expected scale dependent A_{lens} in the ideal, large scale linear limit in Sec. III. For full numerical results we adapt the Boltzmann code MGCAMB in Sec. IV and investigate the lensing power spectrum for several sources of scale dependent physics. We conclude in Sec. V.

II. CMB LENSING POWER SPECTRUM

In this section we give a brief review of CMB lensing and its relation to the matter power spectrum and the gravitational coupling strength. We also illustrate the role of the projection of the matter power from different redshifts and different wave numbers onto the lensing deflection power spectrum observed at a given angular multipole.

As in weak gravitational lensing of background sources such as galaxies, the angular power spectrum of the lensing potential ϕ is given by (see, e.g., [26])

$$C_{\ell}^{\phi\phi} = \frac{8\pi^2}{\ell^3} \int_0^{\chi_{\text{ls}}} d\chi \chi \left(\frac{\chi_{\text{ls}} - \chi}{\chi \chi_{\text{ls}}} \right)^2 P_{\Psi+\Phi} \left(k = \frac{\ell}{\chi}; \chi \right). \quad (1)$$

Here χ is the comoving distance to the lens, χ_{ls} is the comoving distance to the CMB last scattering surface (for simplicity we assume a spatially flat Universe), k is the Fourier wave number, and $P_{\Psi+\Phi}$ is the power spectrum of the sum of the time-time and space-space metric gravitational potentials Ψ and Φ . Thus lensing explicitly depends on cosmic geometry and gravity as well as growth. Note that unlike galaxy lensing, we do not have to integrate over the (inexactly known) source distribution since for the CMB the source is the well-defined last scattering surface. This is an advantage of CMB lensing, in addition to its precision measurements.

Since the lensing potential is not directly observable, we use the deflection vector $\mathbf{d} = \nabla\phi$. This is also related to the convergence $\kappa = -(1/2)\nabla \cdot \mathbf{d} = -(1/2)\nabla^2\phi$. In Fourier space, the power spectra will be related by $C_{\ell}^{\kappa\kappa} = \ell(\ell+1)C_{\ell}^{dd} = [\ell(\ell+1)]^2 C_{\ell}^{\phi\phi}$.

The potential power spectrum can be related to the matter density power spectrum through

$$P_{\Psi+\Phi}(k, z) = \frac{9\Omega_m^2(z)H^4(z)}{8\pi^2} \frac{G_{\text{eff}}^{\Psi+\Phi}(k, z)}{G_N} k^{-1} P_{\delta}(k, z), \quad (2)$$

where $\Omega_m(z)$ is the dimensionless matter density, H is the Hubble parameter, z is the redshift, and G_{eff} reflects that in modified gravity the gravitational strength may not be Newton's G_N , modifying the Poisson equation. A convenient final expression for the convergence power spectrum is [15]

$$C_{\ell}^{\kappa\kappa} = \int dz \frac{H(z)}{\chi^2} W^2(z) P_{\delta}(k = \ell/\chi). \quad (3)$$

Here W is a window function, or kernel. It has a broad peak roughly halfway to the last scattering surface, and so CMB lensing has substantial sensitivity from $z \approx 0.5-5$, allowing it to probe matter and gravity to higher redshifts than many other observables.

[As an aside, note that converting $\Omega_m(a)H^2(z)$ to $\Omega_m H_0^2 a^{-3}$ in Eq. (2) and pulling the present matter density Ω_m outside the integral in Eq. (3) is not valid in models that introduce a matter coupling [27].]

Figure 1 shows the CMB lensing deflection power spectrum for a concordance Λ CDM cosmology, exhibiting the main characteristics (also see the pioneering Figs. 3 and 4 of [26]). While the peak is at $\ell \approx 40$, it extends over a broad range of multipoles. Because of the projection in both redshift and wave number, a given ℓ does not correspond to a unique length scale in the matter power spectrum, or a unique time in the growth of density perturbations. This is important in its effect of blending linear and nonlinear physics.

We indicate what portion of the deflection spectrum arises from lensing in different redshift ranges, and also different Fourier wave numbers. The general rule of thumb is that small k (large scales) corresponds to low ℓ , and low redshift corresponds to large angles for a given scale and hence also low ℓ . However, while high k modes that are beyond the linear regime will dominate the high ℓ spectrum, because of projection ($\ell = k\chi$) they can also influence the lower ℓ region. Thus nonlinear, and scale dependent, physics can leave its mark over a wide range of the deflection power spectrum.

Figure 2 gives one example of the difference that scale dependent physics can make to the redshift and wave

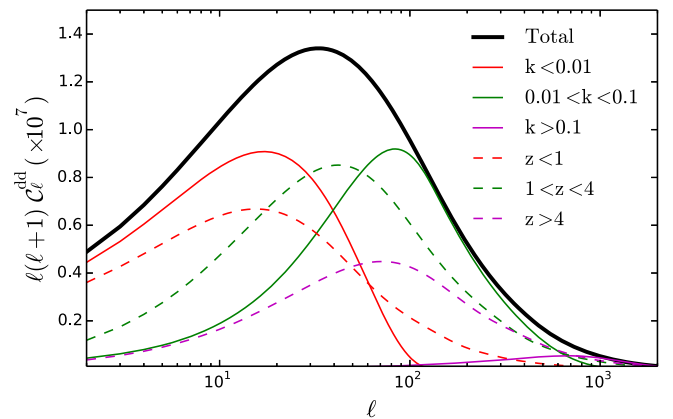


FIG. 1. The lensing deflection power spectrum for a concordance Λ CDM cosmology with $\Omega_m = 0.3$ (main, black curve) is plotted vs multipole, showing a broad peak around the coherence scale of $\sim 2^\circ$, but with power over a range of scattering angles down to the typical deflection of a few arcminutes. The shorter solid curves within the main envelope illustrate the contributions of different Fourier modes k to the deflection spectrum; the dashed curves show the contributions of different redshift windows.

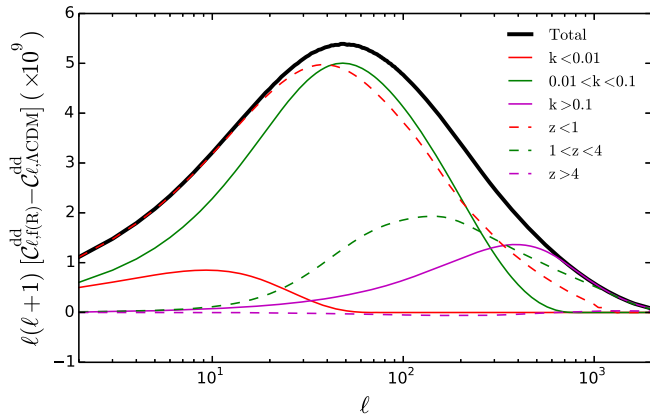


FIG. 2. The deviations in the lensing deflection power spectrum between a Λ CDM and $f(R)$ gravity cosmology are shown for the total power and for various windows in redshift and wave number. Scale dependence can change the redshift and Fourier mode weighting (here exaggerated by taking $B_0 = 0.01$; see Sec. IV for details).

number weighting. This shows the deviation from the Λ CDM case for $f(R)$ scalar-tensor gravity, as discussed in Sec. IV. In this particular case, the contribution from $z < 1$ is most strongly affected since the modified gravity approaches general relativity at high redshift. In wave number, there are different modifications in the low, quasilinear, and high Fourier mode regimes. We give further examples, for different physical origins for scale dependence, in the next section.

III. ANALYTIC SCALE DEPENDENCE

In the linear density perturbation regime, the matter power spectrum in the standard model evolves with a scale independent growth factor, only changing its amplitude. The redshift dependent projection of different Fourier modes k onto multipoles ℓ , however, means that a scale dependence in the lensing power spectrum is induced nevertheless from any change in the growth that arises from a change in the cosmic expansion. (Alteration of growth due purely to a uniform multiplication of the gravitational strength can indeed give a scale independent A_{lens} —indeed this is what [21] originally considered.)

Figure 3 demonstrates this scale dependence. It is generally quite mild, which is why A_{lens} was initially a reasonable parametrization at the signal to noise levels first obtained. We see that the scale dependence is a few percent effect out to $\ell \sim 100$, past the peak of the deflection power spectrum, for a change $\Delta\Omega_m = 0.01$ or $\Delta w = 0.1$, where w is the constant dark energy equation of state parameter. It was only very recently that measurement uncertainties dipped below the 10% level.

Several types of cosmological physics, however, can induce scale dependence in the matter growth even in the linear regime. Examples include modified gravity, such as

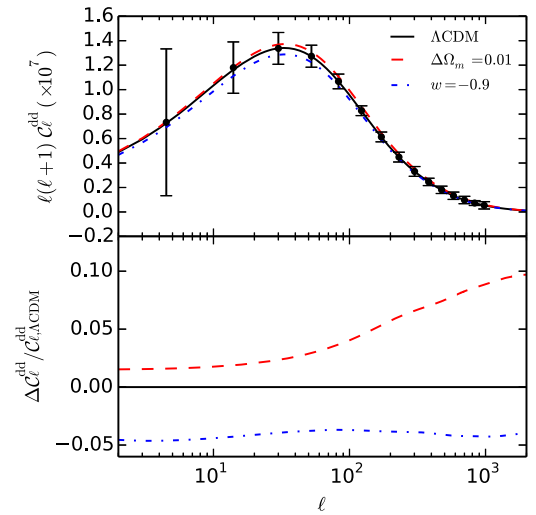


FIG. 3. The effects of changes in the matter density and dark energy constant equation of state on the lensing deflection power spectrum are shown. Since the influence of these parameters on the linear growth factor is scale independent, the resulting deviations in the deflection power spectrum are nearly scale independent—at low ℓ where linear modes are untainted by nonlinear modes. The error bars show uncertainties from Planck 2015 results [10], centered on the Λ CDM theory curve. The current constraints have uncertainties greater than 5%–10% per bandpower and cannot distinguish smaller effects.

scalar-tensor theories, which have a Compton wavelength associated with them, neutrino mass, which has a free streaming scale, and cold (and hence clustered) dark energy, which has a sound horizon. In this section we present a simple analytic treatment purely to build our intuition for the numerical results of the next section.

Note that [28] presents a careful analysis of the effect of the physical matter density on the CMB lensing deflection spectrum. Their fitting formula contains an implicit scale dependence through the local slope of the deflection spectrum. Explicit scale dependent physics from neutrino mass has recently been considered in [29].

As we will see, our results for these cases are in good agreement with theirs, especially taking into account different treatments of the nonlinear regime (they use purely linear modes) and of other parameters (we fix all parameters except the one we are plotting, for clarity in exhibiting its effect; but see Sec. IV regarding preserving the acoustic scale instead).

As our first example of scale dependent physics, consider scalar-tensor gravity. Here the Poisson equation relating the lensing potential $\Psi + \Phi$ to the matter density perturbation is unaffected, but the equation governing the growth of the density is changed. Theories like $f(R)$ gravity involve a particular scale dependence, and the gravitational coupling in the density growth equation can be written as

$$\frac{G_{\text{eff}}^{\Psi}}{G_N} = 1 + \frac{1}{3} \frac{1}{1 + [aM(a)/k]^2}, \quad (4)$$

where M is the mass of the scalaron and $1/M$ its Compton wavelength. On scales larger than the Compton wavelength, the coupling is restored to Newton's constant, or equivalently at early times when the scalaron mass is large then the theory approaches general relativity. On smaller scales, however, gravity is strengthened (while on much smaller scales a chameleon screening mechanism can enter, again restoring to general relativity).

Such changes to the source term of the growth equation can be treated in the formalism of [30] to determine the influence on growth to lowest order. From Eq. (21) of [30], where their $Q(k, a) = G_{\text{eff}}^{\Psi}/G_N$, we have

$$P_{\delta}(k) = P_{\delta, \text{GR}}(k) \left[1 + \int_0^a \frac{da'}{a'} (a'^4 H)^{-1} \times \int_0^{a'} \frac{da''}{a''} \frac{a''^4 H \Omega_m(a'')}{1 + [a''M(a'')/k]^2} \right]^2 \quad (5)$$

$$\approx P_{\delta, \text{GR}}(k) \left[1 + k^2 \int_0^a \frac{da'}{a'} (a'^4 H)^{-1} \times \int_0^{a'} \frac{da''}{a''} \frac{a''^2 H \Omega_m(a'')}{M^2} \right] \quad (6)$$

$$\approx P_{\delta, \text{GR}}[1 + k^2 p(a)]. \quad (7)$$

The last two lines with the approximate signs keep only the lowest order terms in k , with the last line illustrating the leading order k^2 dependence of the modification. (Sound horizon terms also enter as k^2 , while neutrino free streaming gives a different dependence but the general formalism still applies.) From Eq. (3) we note that an additional k^2 term in $P_{\delta}(k)$ does not simply create an additional ℓ^2 modification of the lensing power spectrum. Instead it reweights C_{ℓ} from the mass power spectrum at each redshift. That is,

$$\frac{C_{\ell}^{dd}}{\bar{C}_{\ell}^{dd}} = 1 + \frac{\ell^2}{\bar{C}_{\ell}^{dd}} \int dz \frac{H(z)}{\chi^2} W^2(z) \bar{P}_{\delta} \frac{p(z)}{\chi^2} \approx 1 + \left\langle \frac{p(z)}{\chi^2} \right\rangle \quad (8)$$

where a bar indicates the unmodified (GR) case and angle brackets indicate a weighting over redshift, accounting for $k = \ell/\chi$. This is an important point, and means that scale dependent physics does not necessarily have an obvious form.

Where might we expect the largest modification in the deflection power spectrum? This will be addressed numerically in the next section but here we can gain some intuition. Modified gravity that is consistent with other

observations becomes important only fairly recently. For example, from Fig. 6 of [31] we see that a modification in the matter spectrum by 10% today may have been less than 1% at $z = 1$. Equivalently, Fig. 5 of [31] shows that the parameter B related to the Compton wavelength can easily be one to two orders of magnitude smaller at $z = 1$ than its value B_0 today. As discussed previously, low redshift lensing contributed most to low multipoles, but so do low k modes where the modification is suppressed by k^2 . Conversely, higher k modes where modified gravity effects are more important should appear at high ℓ , but here one also has high redshift lensing contributions where modified gravity is diminished. Thus, the modified contributions are diluted by the unmodified ones. Since there are many more high k modes than low k ones, one might expect that the modifications do grow with ℓ , but much more slowly than a naive $k^2 \rightarrow \ell^2$ scaling, and that a low ℓ tail should be present. At high enough ℓ (roughly Mpc scales, and low redshift, so $\ell \gtrsim 10^3$), the screening mechanism should enter and the deflection power spectrum approach that of Λ CDM. The numerical computations bear this out.

Let us further our intuition for the results by briefly considering neutrino mass, cold (clustered) dark energy, and standard matter density nonlinearities. If we compare models with different sums of the neutrino masses, we have to specify how we are compensating for this energy density in order to retain a total dimensionless energy density of unity, i.e. a spatially flat universe. If we trade matter density ($\Omega_m h^2$) for neutrino mass, then on large scales the non-relativistic neutrinos act in the same manner as the subtracted matter, and we expect no significant effect. However on small scales, where the neutrinos free stream, we not only erase gravitational potentials from the free streaming but also reduce the matter clustering since there is less matter; these effects together should reinforce each other to cause substantial suppression of the deflection power spectrum. If the extra neutrino mass is compensated by reduced dark energy density ($\Omega_{\Lambda} h^2$), then the neutrino free streaming is replacing what would anyway have been suppression due to the dark energy negative pressure, and so the effect should be more mild.

Figure 4 illustrates how the lensing deflection power spectrum changes due to the presence of massive neutrinos for the case of matter compensated neutrino mass. The results are fairly similar in the case of dark energy compensated neutrino mass except that, as stated above, the matter compensated case has a stronger effect. Most of the change in power due to neutrino mass is on intermediate scales near the free streaming scale. This, together with the projection between k and ℓ , explains the pattern seen in the figure.

As for dark energy, it can only clump on scales between the sound horizon and the Hubble scale, so a low sound speed (cold dark energy) is necessary for its clumping (as well as an equation of state significantly different from

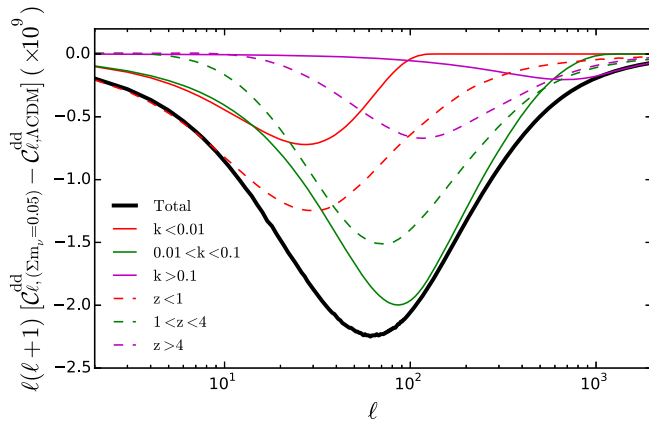


FIG. 4. The deviations in the lensing deflection power spectrum between Λ CDM and a model where part of the CDM energy density is replaced with that of massive neutrinos with $\sum m_\nu = 0.05$ eV are shown for the total power and for various windows in redshift and wave number. The CMB lensing power is suppressed due to neutrino free streaming and less CDM clustering. A similar trend exists for the case where part of the dark energy density is replaced with that of massive neutrinos.

$w = -1$ at some epoch). If the dark energy clusters it can add to the deflection power, and furthermore the value of $w \neq -1$ removes some of the suppression of power, so cold (clustered) dark energy could leave an enhancement signature in the deflection power spectrum at low ℓ .

Figure 5 summarizes these effects. It can be seen that the influence is predominantly on large scales ($k < 0.1$ h/Mpc), where the additional clustering enhances the deflection power spectrum. Moreover this is mostly relevant at low redshift ($z < 1$) when dark energy dominates the energy budget of the Universe.

Finally, density perturbation growth beyond the linear regime exhibits scale dependence. This enters at $k \gtrsim 0.1$ h/Mpc in the matter power spectrum, which normally

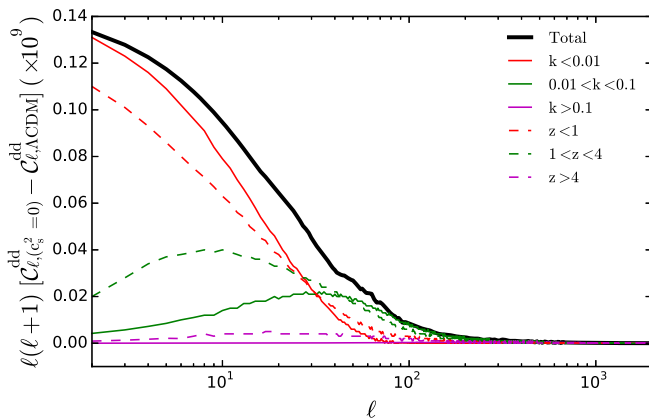


FIG. 5. The deviations in the lensing deflection power spectrum between Λ CDM and a cold dark energy model are shown for the total power and for various windows in redshift and wave number. In this case the CMB lensing power is enhanced, mostly on large scales and at late times.

we would translate to roughly $\ell \gtrsim 1000$. However, we expect that due to projection effects even lower ℓ can show noticeable effects. (See Fig. 1, where the total power begins to diverge from the $k < 0.1$ power around $\ell \approx 200$, and even sooner for higher Ω_m .) In addition, nonlinearity is more prevalent at low redshifts, also pushing the influence to lower ℓ . We will address this numerically in the next section.

IV. NUMERICAL SCALE DEPENDENCE

To explore all these effects we carry out a full numerical computation using the Boltzmann code MGCAMB (see [32,33] for details). MGCAMB is a modified version of the CAMB code [34] which includes a general parametrization of modified gravity theories in the linear regime of perturbations. This will enable us to investigate the scale dependence of C_ℓ^{dd} in the cases of modified gravity theories, neutrino mass, and cold (low sound speed) dark energy.

As a specific modified gravity theory we choose $f(R)$ models with the action

$$S = \frac{1}{16\pi G} \int d^4x \sqrt{-g} [R + f(R) + \mathcal{L}_m]. \quad (9)$$

These models can be tuned to reproduce any background expansion history, and the remaining relevant quantity is the squared Compton wavelength of the new scalar degree of freedom $f_R \equiv df/dR$ mediating the fifth force. In units of the Hubble length squared it is given by [35,36]

$$B \equiv \frac{f_{RR}}{1 + f_R} \frac{dR}{d \ln a} \left(\frac{d \ln H}{d \ln a} \right)^{-1}. \quad (10)$$

For a fixed background expansion history, different $f(R)$ models can be parametrized by the parameter B_0 , which is related to the present value of the scalaron parameter $f_{R0} \approx -B_0/5$. The exact relation depends on the specific $f(R)$ model.

Note that because of the rapid evolution of the curvature, a small value $B(z)$ could correspond to a much larger B_0 or f_{R0} . For example, in the exponential gravity model [31] $B_0 = 0.01$ could come from $B(z = 1) = 10^{-4}$, and hence show little growth modification at high redshift. Regarding the expansion history, the maximum deviation of the dark energy equation of state $|1 + w_{\max}| \approx B_0/2$ for exponential gravity, essentially giving Λ CDM behavior. For examples of these relations, see Fig. 5 of [31]. Thus, not all modified gravity theories will give clear signatures in early growth or in expansion. We consider instead a commonly used model, essentially the easiest case to constrain: Hu-Sawicki $f(R)$ gravity with $n = 1$ [36]. As n gets larger, B evolves more rapidly, similar to the exponential gravity case, and becomes harder to constrain.

In evaluating modified gravity effects it is important to use a robust code and not assume aspects of standard Λ CDM growth. MGCAMB has been tested against an independent Boltzmann code EFTCAMB [37], for example in [38], and the results are in good agreement. While MGCAMB evaluates the evolution equations in the quasi-static limit (while EFTCAMB treats them generally), this is an excellent approximation on the scales of interest to us [39–41]. The lensing analysis in [42] also confirms that the quasistatic approximation is good. MGCAMB can also, in principle, include the nonlinear matter power spectrum unlike the intrinsically linear EFTCAMB formalism. We have seen that nonlinearities enter already at $\ell \approx 200$. To incorporate the nonlinear density behavior for the $f(R)$ model, we employ the MGHaloFit patch [43], which has been calibrated from simulations to correctly account for the modified gravity effects.

Figure 6 compares the CMB lensing power spectra of the scale dependent models discussed in the previous section to that from the fiducial (Λ CDM) model. In the $f(R)$ modified gravity model, we see an enhancement of power (as expected since scalar-tensor theories strengthen the gravitational coupling) on all scales. At low multipoles the effect is weaker, since on large scales, greater than the Compton wavelength, the coupling approaches Newton’s constant [see Eq. (4)]. At high multipoles (which recall include very nonlinear scales), the chameleon screening enters and again the result goes toward the general relativity case. Thus the expectation of Sec. III is borne out: the power approaches

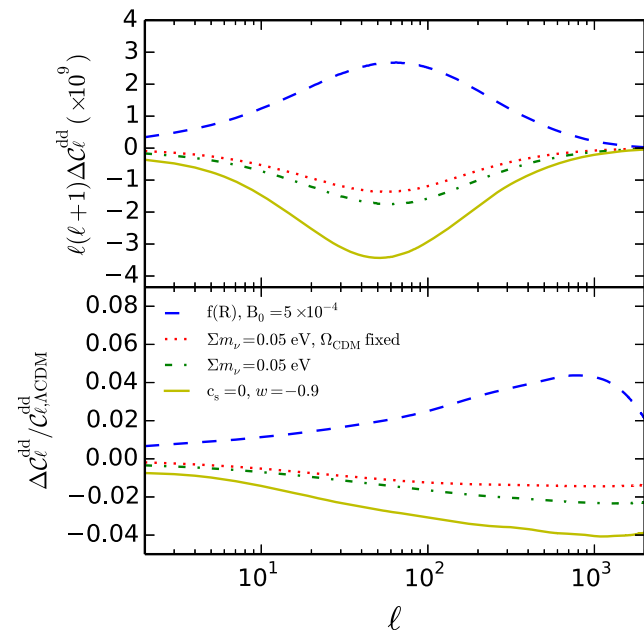


FIG. 6. The CMB lensing deflection power spectrum is plotted vs multipole ℓ for several models with scale dependent physics, including modified gravity with a Compton scale B_0 , neutrinos with a sum of masses $\sum m_\nu$, and cold dark energy with a sound speed c_s .

the Λ CDM value on scales above the scalaron wavelength and below the screening scale. However in general we see a modification of CMB lensing power over a wide range of ℓ from a range of redshifts.

For the impact of massive neutrinos, recall we distinguished two cases. When we add massive neutrinos and keep $\Omega_m h^2$ fixed (retaining spatial flatness by decreasing Λ), we see that free streaming suppresses lensing power at small scales, smaller than the free streaming scale, as expected. However, when the added energy density of the massive neutrinos is compensated by decreasing that of the CDM instead, the effect is more pronounced on all scales. Not only is there suppression from free streaming but there is also less clustering due to the lower Ω_m .

Scale dependence can also arise due to density perturbations above the sound horizon of cold dark energy with a low sound speed. As predicted in Sec. III the effects of low sound speed enter at low multipoles. At higher multipoles, [44] showed that one could rescale the CMB lensing deflection spectrum by a uniform factor A_{lens} to a good approximation to take into account the deviation of w from Λ . This agrees well with Fig. 3, where we see that the deviation in power due to $w \neq -1$ is almost perfectly scale independent. If in Fig. 6 one adjusted the high multipoles to match Λ CDM, then the low multipoles show the expected power gain due to the clustering of cold dark energy. We make this more explicit in Fig. 7.

Note that the shapes of the deviations in the CMB lensing spectrum are distinct between the different scale

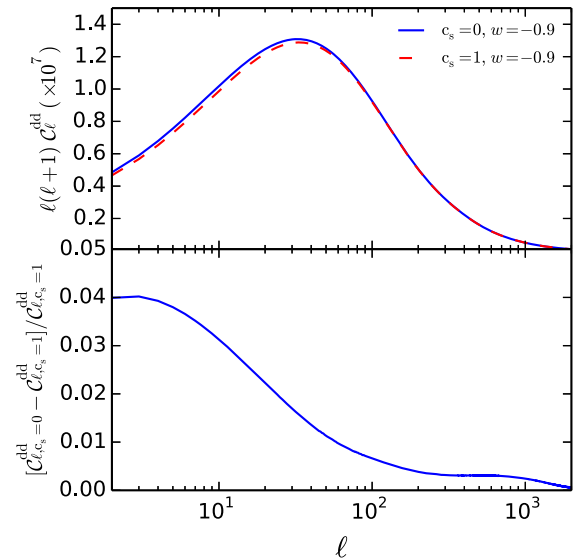


FIG. 7. Cold dark energy provides extra clustering, and hence deflection power, on scales larger than the sound horizon (hence low multipoles). This also leads to scale dependence in the ratio of the power to that of Λ CDM, or quintessence. The bottom panel shows the deviation of cold dark energy from quintessence with the same value $w = -0.9$, but $c_s = 1$.

dependent physics. Modified gravity gives a rise and fall, while neutrino mass leads to an almost tanh-like behavior of a low ℓ plateau, then nearly linear slope, then a high ℓ plateau, and cold dark energy gives a slightly more curved version of this, and one that is not scale independent at high ℓ . (We have checked that a change in the Hubble constant to preserve the CMB acoustic scale does not appreciably change the shapes though it does increase the amplitude of the deviations.)

The differing scale dependences would allow for identification of the non- Λ CDM physics with sufficiently precise measurements. Here we have concentrated solely on the deflection power spectrum. These effects of course also show up in the matter power spectrum (which causes the deflections) but there the measurement through galaxy surveys has to contend with the expected scale dependent galaxy bias. CMB lensing also affects other CMB power spectra, giving secondary contributions to them involving the extra physics, though these will be mixed with the (unlensed) primordial perturbations.

However, we highlight in Fig. 8 a very interesting property of the E -mode spectrum: at high multipoles it is almost wholly due to lensing. This holds independent of the details of the physics modifications we discussed in this paper. As an example, Fig. 8 demonstrates the same conclusion in the case of the modified gravity models as well. High resolution CMB polarization experiments with ~ 1 arcmin beams can reach $\ell = 10000$ and our current knowledge indicates that the E -mode polarization signals should not be overwhelmed by foreground polarization, so this could be a promising avenue for exploration.

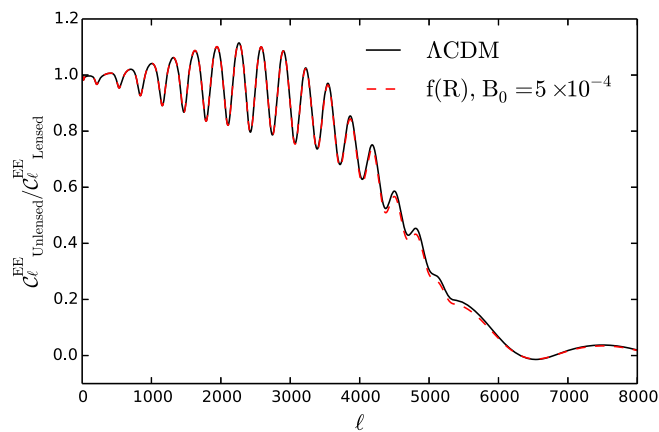


FIG. 8. CMB lensing smears out the acoustic peaks, causing oscillatory enhancements and dilutions of the unlensed, primordial power. However, it also converts the higher amplitude T modes into E -mode polarization, in particular on the characteristic scattering scale of $\sim 2'$. This leads to almost all the E -mode power at $\ell > 5000$ being due to CMB lensing. The black curve shows the ratio of unlensed to lensed E -mode power as a function of multipole for a Λ CDM cosmology, while the dashed, red curve shows that the same behavior holds in $f(R)$ gravity.

V. CONCLUSIONS

CMB lensing is a unique probe of the physics driving both expansion and growth over vast ranges of cosmic history, sensitive to $z \approx 5$ and beyond. Experimental measurements are approaching percent precision in dozens of multipole bins, and now- or imminently operating high resolution CMB polarization experiments such as ACTpol, POLARBEAR/Simons Array, and SPT-3G, and the next generation CMB-S4, can achieve this over large areas of sky. This opens windows on physics beyond that mapped by the temperature power spectrum, or unlensed polarization. Here we focused on physics that introduces a new scale, such as modified gravity, massive neutrinos, and cold dark energy.

We explored the signatures of this physics, first through analytic approximations to build intuition on the effects, and then through rigorous numerical calculations, for example using a modified gravity Boltzmann code and nonlinear prescription calibrated by simulations. The analytic intuition works well at predicting the areas and qualitative behavior of deviation from Λ CDM in the CMB lensing deflection power spectrum.

Moreover, the shapes (angular dependence) of the deviations are fairly distinct between the various scale dependent physics origins. Sufficiently accurate measurements thus have the promise of distinguishing the nature of the physics behind detected deviations—i.e. measuring the gravitational coupling G_{eff} , the sum of neutrino masses $\sum m_\nu$, or the dark energy sound speed c_s . While hints of scale dependent variation are seen in current data, they are not yet statistically significant.

For modified gravity, we found that $f(R)$ gravity with $f_{R0} \approx 10^{-4}$ could give a deviation roughly the same in amplitude as a shift in the matter density of $\Delta\Omega_m = 0.01$. Due to the projection of wavemodes, it is crucial by $\ell \approx 200$ already to treat the nonlinear wave numbers consistently, which we did using MGhalofit. Other recent applications of CMB lensing to test gravity (not necessarily scale dependence, as we focus on here) include [45,46]. Neutrino masses, even at the level of $\sum m_\nu = 0.05$ eV, also give a couple of percent signal, with a characteristic shape. Cold dark energy only distinguishes itself from quintessence at low multipoles, where cosmic variance dominates.

Neglecting to account for scale dependent physics despite its presence will generally bias other cosmological parameter estimation. This can also be an issue for delensing of B -modes: if the poorly reconstructed parts of the deflection spectrum (and their contributions to the B -mode lensing polarization) are employed assuming some model that lacks existing scale dependence, this can bias the fit of the tensor to scalar ratio r of inflation.

The scale dependent physics will also show up in other power spectra. For the galaxy power spectrum this may be difficult to separate from scale dependent galaxy bias, small scale nonlinearities, and baryonic effects. Other CMB power spectra have the lensing contributions mixed with the

primordial spectra. However, with the advance of high resolution CMB polarization experiments capable of reaching $\ell = 10000$, and the hint that polarized foregrounds are small enough for such arcminute scale data to be useful, it is exciting to note that E -mode polarization at $\ell \gtrsim 5000$ is almost purely due to CMB lensing. CMB lensing, and its E - and B -mode contributions, is an arena capable of offering new physics insights beyond the concordance model.

ACKNOWLEDGMENTS

We thank Antony Lewis and Blake Sherwin for helpful discussions. A. H. is supported by a NSERC postdoctoral fellowship. E. L. is supported by the U.S. Department of Energy, Office of Science, Office of High Energy Physics, under Award No. DE-SC-0007867 and Contract No. DE-AC02-05CH11231.

-
- [1] E. V. Linder, *Astron. Astrophys.* **206**, 199 (1988).
 [2] S. Cole and G. Efstathiou, *Mon. Not. R. Astron. Soc.* **239**, 195 (1989).
 [3] M. Sasaki, *Mon. Not. R. Astron. Soc.* **240**, 415 (1989).
 [4] E. V. Linder, *Mon. Not. R. Astron. Soc.* **243**, 362 (1990).
 [5] S. Das *et al.*, *Phys. Rev. Lett.* **107**, 021301 (2011).
 [6] M. Zaldarriaga and U. Seljak, *Phys. Rev. D* **59**, 123507 (1999).
 [7] T. Okamoto and W. Hu, *Phys. Rev. D* **67**, 083002 (2003).
 [8] M. Zaldarriaga and U. Seljak, *Phys. Rev. D* **58**, 023003 (1998).
 [9] Planck Collaboration, *Astron. Astrophys.* **571**, A17 (2014).
 [10] Planck Collaboration, arXiv:1502.01591.
 [11] A. van Engelen *et al.*, *Astrophys. J.* **808**, 7 (2015).
 [12] A. van Engelen *et al.*, *Astrophys. J.* **756**, 142 (2012).
 [13] D. Hanson *et al.*, *Phys. Rev. Lett.* **111**, 141301 (2013).
 [14] R. Keisler *et al.*, *Astrophys. J.* **807**, 151 (2015).
 [15] POLARBEAR Collaboration, *Phys. Rev. Lett.* **112**, 131302 (2014).
 [16] POLARBEAR Collaboration, *Phys. Rev. Lett.* **113**, 021301 (2014).
 [17] POLARBEAR Collaboration, *Astrophys. J.* **794**, 171 (2014).
 [18] BICEP2/Keck Array and Planck Collaborations, *Phys. Rev. Lett.* **114**, 101301 (2015).
 [19] S. Das *et al.*, *J. Cosmol. Astropart. Phys.* 04 (2014) 014.
 [20] K. T. Story *et al.* (SPT Collaboration), *Astrophys. J.* **810**, 50 (2015).
 [21] E. Calabrese, A. Slosar, A. Melchiorri, G. F. Smoot, and O. Zahn, *Phys. Rev. D* **77**, 123531 (2008).
 [22] Planck Collaboration, arXiv:1507.02704.
 [23] M. Niemack *et al.*, *Proc. SPIE Int. Soc. Opt. Eng.* **7741**, 77411S (2010); <http://www.princeton.edu/act>.
 [24] Z. Kermish *et al.*, *Proc. SPIE Int. Soc. Opt. Eng.* **8452**, 84521C (2012); T. Tomaru *et al.*, *Proc. SPIE Int. Soc. Opt. Eng.* **8452**, 84521H (2012); <http://bolo.berkeley.edu/polarbear>.
 [25] J. Austermann *et al.*, *Proc. SPIE Int. Soc. Opt. Eng.* **8452**, 84521E (2012); <http://pole.uchicago.edu>.
 [26] A. Lewis and A. Challinor, *Phys. Rep.* **429**, 1 (2006).
 [27] S. Das, R. de Putter, E. V. Linder, and R. Nakajima, *J. Cosmol. Astropart. Phys.* 11 (2012) 011.
 [28] Z. Pan, L. Knox, and M. White, *Mon. Not. R. Astron. Soc.* **445**, 2941 (2014).
 [29] Z. Pan and L. Knox, arXiv:1506.07493.
 [30] E. V. Linder and R. N. Cahn, *Astropart. Phys.* **28**, 481 (2007).
 [31] E. V. Linder, *Phys. Rev. D* **80**, 123528 (2009).
 [32] A. Hojjati, L. Pogosian, and G.-B. Zhao, *J. Cosmol. Astropart. Phys.* 08 (2011) 005.
 [33] A. Hojjati, *J. Cosmol. Astropart. Phys.* 01 (2013) 009.
 [34] A. Lewis, A. Challinor, and A. Lasenby, *Astrophys. J.* **538**, 473 (2000); <http://camb.info>.
 [35] Y.-S. Song, W. Hu, and I. Sawicki, *Phys. Rev. D* **75**, 044004 (2007).
 [36] W. Hu and I. Sawicki, *Phys. Rev. D* **76**, 064004 (2007).
 [37] B. Hu, M. Raveri, N. Frusciante, and A. Silvestri, *Phys. Rev. D* **89**, 103530 (2014).
 [38] M. Raveri, B. Hu, N. Frusciante, and A. Silvestri, *Phys. Rev. D* **90**, 043513 (2014).
 [39] A. Hojjati, L. Pogosian, A. Silvestri, and S. Talbot, *Phys. Rev. D* **86**, 123503 (2012).
 [40] A. Hojjati, L. Pogosian, A. Silvestri, and G. B. Zhao, *Phys. Rev. D* **89**, 083505 (2014).
 [41] S. Bose, W. A. Hellwing, and B. Li, *J. Cosmol. Astropart. Phys.* 02 (2015) 034.
 [42] Planck Collaboration, arXiv:1502.01590.
 [43] G. B. Zhao, *Astrophys. J. Suppl. Ser.* **211**, 23 (2014).
 [44] E. Calabrese, A. Cooray, M. Martinelli, A. Melchiorri, L. Pagano, A. Slosar, and G. F. Smoot, *Phys. Rev. D* **80**, 103516 (2009).
 [45] A. R. Pullen, S. Alam, and S. Ho, *Mon. Not. R. Astron. Soc.* **449**, 4326 (2015).
 [46] B. Hu and M. Raveri, *Phys. Rev. D* **91**, 123515 (2015).